6-19-2009

Aintegumenta and *Aintegumenta-Like6* Act Redundantly to Regulate Arabidopsis Floral Growth and Patterning

Beth A. Krizek
University of South Carolina - Columbia, krizek@sc.edu

Publication Info

Published in *Plant Physiology*, ed. Donald R. Ort, Volume 150, Issue 4, 2009, pages 1916-1929.

AINTEGUMENTA and *AINTEGUMENTA-LIKE6* Act Redundantly to Regulate Arabidopsis Floral Growth and Patterning[1][C][W][OA]

Beth A. Krizek*

Department of Biological Sciences, University of South Carolina, Columbia, South Carolina 29208

An Arabidopsis (*Arabidopsis thaliana*) flower consists of four types of organs arranged in a stereotypical pattern. This complex floral structure is elaborated from a small number of floral meristem cells partitioned from the shoot apical meristem during reproductive development. The positioning of floral primordia within the periphery of the shoot apical meristem depends on transport of the phytohormone auxin with floral anlagen arising at sites of auxin maxima. An early marker of lateral organ fate is the AP2/ERF-type transcription factor AINTEGUMENTA (ANT), which has been proposed to act downstream of auxin in organogenic growth. Here, I show that the related, *AINTEGUMENTA-LIKE6* (*AIL6*)/*PLETHORA3* gene acts redundantly with *ANT* during flower development. *ant ail6* double mutants show defects in floral organ positioning, identity, and growth. These floral defects are correlated with changes in the expression levels and patterns of two floral organ identity genes, *APETALA3* and *AGAMOUS*. *ant ail6* flowers also display altered expression of an auxin-responsive reporter, suggesting that auxin accumulation and/or responses are not normal. Furthermore, I show that *ANT* expression in incipient and young floral primordia depends on auxin transport within the inflorescence meristem. These results show that *ANT* and *AIL6* are important regulators of floral growth and patterning and that they may act downstream of auxin in these processes.

During reproductive development in Arabidopsis (*Arabidopsis thaliana*), floral meristems are initiated reiteratively from groups of cells within the periphery of the shoot apical meristem. The particular sites at which flowers are initiated correspond to local auxin maxima generated by polar transport of the hormone by efflux carriers such as PINFORMED1 (PIN1; for review, see Fleming, 2007). Two genes closely associated with floral initiation are *LEAFY* (*LFY*) and *AINTEGUMENTA* (*ANT*), which act in the specification of floral meristem identity and growth, respectively. Both genes are expressed in incipient floral anlagen prior to outgrowth, and their expression patterns are altered in *pin1* mutants, which are defective in floral initiation (Weigel et al., 1992; Elliott et al., 1996; Vernoux et al., 2000). The inability of *pin1* mutants to initiate flowers can be rescued by the application of auxin paste to the periphery of the shoot apex, demonstrating the necessity and sufficiency of auxin for lateral organ development (Reinhardt et al., 2000).

Once established, floral meristems give rise to floral organ primordia at spatially defined positions within four concentric whorls. In an Arabidopsis flower, four sepal primordia arise in the outer first whorl, four petal primordia arise in the second whorl, six stamen primordia arise in the third whorl, and two carpel primordia arise in the centermost fourth whorl. Four different classes of floral organ identity genes (A, B, C, and E) act in different regions of the flower to specify these different organ identities (for review, see Krizek and Fletcher, 2005). The class A genes *APETALA1* (*AP1*) and *AP2* are active in whorls one and two; the class B genes *AP3* and *PISTILLATA* are active in whorls two and three; the class C gene *AGAMOUS* (*AG*) is active in whorls three and four; and the E class, consisting of *SEPALLATA1* (*SEP1*) to *SEP4*, is active in all four whorls. The region-specific activities of the class A, B, and C genes result primarily from regulation at the level of transcription. *LFY* encodes a novel transcription factor with similarity to helix-turn-helix proteins (Hames et al., 2008) that is expressed throughout stage 1 and 2 floral meristems (Weigel et al., 1992). The broadly expressed LFY acts in combination with different regionally expressed coregulators to activate the floral organ identity genes in distinct subdomains within the flower (Parcy et al., 1998). In the case of *AG* activation, LFY acts in combination with the homeodomain protein WUSCHEL (WUS), an important regulator of stem cell identity (Lenhard et al., 2001; Lohmann et al., 2001). *AG* activity later feeds back to down-regulate *WUS* expression in the center of the flower, resulting in termination of the floral meristem (Lenhard et al., 2001; Lohmann et al., 2001).

[1] This work was supported by the U.S. Department of Energy (grant no. 98ER20312).

* E-mail krizek@sc.edu.

The author responsible for distribution of materials integral to the findings presented in this article in accordance with the policy described in the Instructions for Authors (www.plantphysiol.org) is: Beth A. Krizek (krizek@sc.edu).

[C] Some figures in this article are displayed in color online but in black and white in the print edition.

[W] The online version of this article contains Web-only data.

[OA] Open Access articles can be viewed online without a subscription.

www.plantphysiol.org/cgi/doi/10.1104/pp.109.141119

Despite our knowledge about the control of floral organ identity and floral determinacy, other aspects of floral development remain obscure at the mechanistic level. This is especially true of early floral meristem patterning events such as floral organ positioning and primordia outgrowth. These processes are likely to be regulated by auxin because of their analogy with lateral organ positioning and primordium outgrowth from the shoot apical meristem. However, floral meristems are determinate, whereas the shoot apical meristem exhibits indeterminate growth. In addition, floral organ primordia arise in a whorled rather than a spiral phyllotaxis, thus requiring the simultaneous generation of multiple auxin maxima within the floral meristem. There is limited information on auxin distribution in early stages of flower development (Benkova et al., 2003; Heisler et al., 2005), and genes that act downstream of auxin in floral meristem patterning have not been identified. In later stages of flower development, auxin accumulates in the tips of developing floral primordia, where it is thought to specify a new growth axis (Benkova et al., 2003).

ANT is an important regulator of growth during lateral organ development. *ant* flowers reach a smaller final size, while plants constitutively expressing *ANT* produce flowers that reach a larger final size (Elliott et al., 1996; Klucher et al., 1996; Krizek, 1999; Mizukami and Fischer, 2000). Several pieces of evidence link ANT function in organ growth with auxin signaling. *ANT* acts downstream of the novel auxin-inducible gene *ARGOS* (for auxin-regulated gene involved in organ size; Hu et al., 2003). Similar to *ANT*, loss- and gain-of-function *ARGOS* plants display opposite effects on lateral organ growth, and *ANT* activity is required for the increased size of lateral organs in *35S:ARGOS* plants (Hu et al., 2003). Furthermore, *ANT* expression in maturing organs may be negatively regulated by *AUXIN RESPONSE FACTOR2* (*ARF2*), a repressor of organ growth (Schruff et al., 2005).

ANT is a member of the large AP2/ERF transcription factor family, containing a DNA-binding domain that corresponds to two AP2 repeats and the conserved intervening linker region (Nole-Wilson and Krizek, 2000). Seven AINTEGUMENTA-like (AIL)/PLETHORA (PLT) proteins share high sequence similarity to ANT within this DNA-binding domain, but as a group these eight proteins do not share sequence similarity outside of this region (Nole-Wilson et al., 2005). High amino acid similarity is found throughout the sequences of two pairs of AIL/PLT proteins (AIL6/PLT3 and AIL7, PLT1 and PLT2; Fig. 1A). *ANT*, *AIL5*, *AIL6/PLT3*, and *AIL7* show partially overlapping but distinct expression patterns within the inflorescence meristem and developing flowers, suggesting that these genes may function redundantly during flower development (Nole-Wilson et al., 2005). Four *AIL/PLT* genes (*PLT1*, *PLT2*, *AIL6/PLT3*, and *BBM*) have been shown to act redundantly in root development (Aida et al., 2004; Galinha et al., 2007).

Here, I show that *AIL6* acts redundantly with *ANT* during shoot development. While *ail6* single mutants display no obvious morphological differences from the wild type, *ant ail6* double mutants show defects during both vegetative and reproductive development. *ant ail6* flowers exhibit altered positioning of floral organ primordia, loss of floral organ identity, and reduced growth of floral organ primordia. These defects are correlated with altered expression of stem cell and floral regulatory genes as well as the auxin-responsive reporter *AGH3-2:GUS*. *ANT* expression in incipient and young floral primordia is reduced after treatment with the auxin transport inhibitor *N*-1-naphthylphthalamic acid (NPA), thus suggesting a role for auxin transport in the regulation of *ANT* expression. These results support a model in which *ANT* and *AIL6* promote growth and patterning in flowers downstream of auxin.

RESULTS

ail6 and *ail6 ail7* Mutants Have a Wild-Type Appearance

To investigate the function of *AIL6* (At5g10510), I identified four T-DNA insertion lines (Fig. 1B; Krysan et al., 1999; Sessions et al., 2002; Alonso et al., 2003; Rosso et al., 2003). The T-DNAs are present in the second intron (WISC 475_E04, *ail6-3*), third intron (SALK_127417, *ail6-1/plt3-1*; SAIL 690_B11, *ail6-2*), and sixth exon (Gabi-Kat 765_G02, *ail6-4*) of *AIL6*. None of these lines display any obvious morphological differences compared with the wild type during either vegetative or reproductive development (Fig. 1, D–G). *AIL6* expression levels were examined in three of these T-DNA lines by in situ hybridization using a probe directed against the second exon of *AIL6* (Fig. 1B). *AIL6* mRNA levels were significantly reduced in *ail6-1*, *ail6-2*, and *ail6-3* inflorescences as compared with Columbia (Col) wild-type inflorescences (Fig. 1, J and K; data not shown). The weak signal detectable in *ail6-2* inflorescences (Fig. 1K) suggests that a partial transcript that includes exon 2 is produced in this allele.

To determine if *AIL6* might act redundantly with the closely related gene *AIL7*, I identified a single T-DNA line carrying an insertion within *AIL7* (SAIL 1167_C10, *ail7-1*; Fig. 1C). The T-DNA is present in the sixth exon of *AIL7*. While partial transcripts have been detected in *ail7-1* plants (J. Mudunkothge and B. Krizek, unpublished data), it is likely that any protein produced in these plants is nonfunctional, as the T-DNA is present within sequences encoding the linker between the two AP2 domains. *ail7-1* plants have a wild-type appearance (Fig. 1H). *ail6-2* was crossed to *ail7-1* to generate the double mutant, which also exhibited no obvious morphological differences compared with wild-type plants (Fig. 1I).

ant ail6 Flowers Display Reduced Petal, Stamen, and Carpel Identities

AIL6 is more distantly related to *ANT*, but previously published in situ hybridization experiments

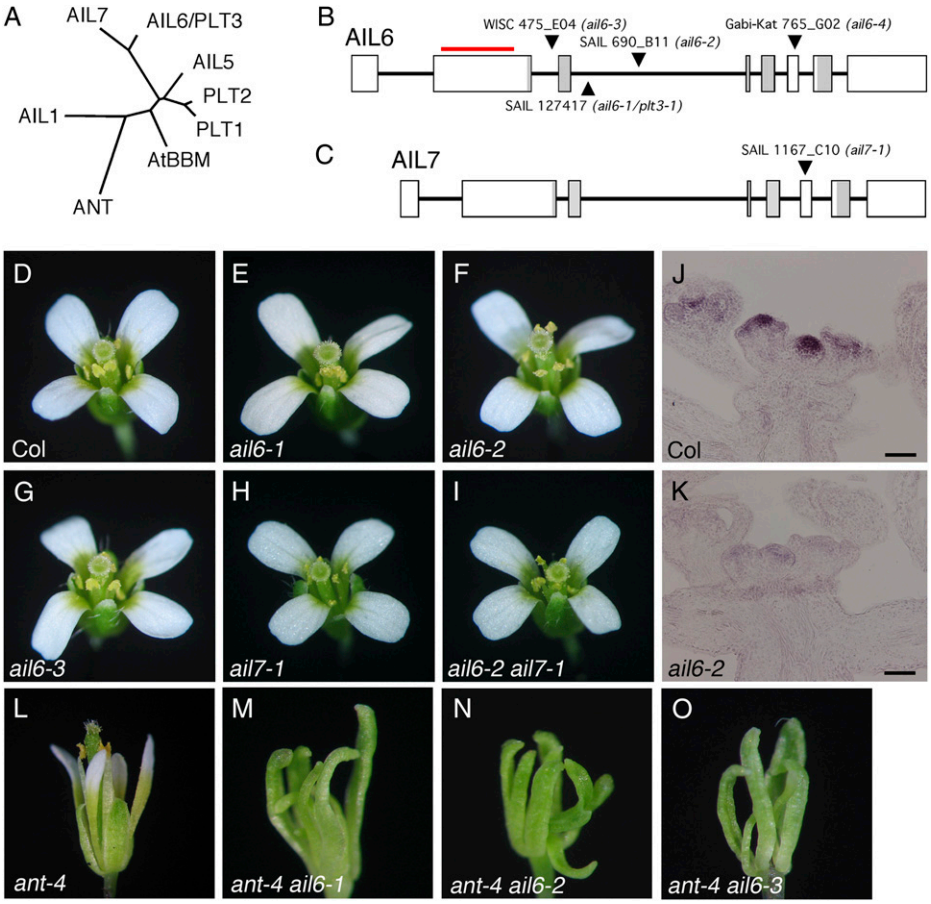

Figure 1. *ail6*, *ail7*, *ail6 ail7*, and *ant ail6* flowers. A, Phylogenetic tree showing the relationship between AIL proteins. B and C, Genomic structures of *AIL6* (B) and *AIL7* (C). Boxes indicate exons, with gray shading marking the two AP2 domains. The red bar shows the region of *AIL6* used as an in situ hybridization probe. The positions of the insertions in the T-DNA alleles are shown with triangles. D, Col flower. E, *ail6-1* flower. F, *ail6-2* flower. G, *ail6-3* flower. H, *ail7-1* flower. I, *ail6-2 ail7-1* flower. J and K, *AIL6* expression in wild-type (J) and *ail6-2* (K) inflorescences. L, *ant-4* flower. M, *ant-4 ail6-1* flower. N, *ant-4 ail6-2* flower. O, *ant-4 ail6-3* flower. Images in D to F and G to I are shown at the same magnification. Bars = 50 μm in J and K.

showed that these two genes are expressed in partially overlapping domains in inflorescences (Elliott et al., 1996; Nole-Wilson et al., 2005). To investigate whether *AIL6* function overlaps with that of *ANT*, the strong *ant-4* allele in the Landsberg *erecta* (L*er*) background (Baker et al., 1997; Nole-Wilson and Krizek, 2006) was crossed to all four *ail6* alleles. All of these double mutants displayed a similar enhanced phenotype compared with *ant-4* single mutants (Fig. 1, L–O). This double mutant phenotype is not significantly affected by the mixed Col/L*er* background (Supplemental Fig. S1). A detailed phenotypic characterization of the *ant-4 ail6-2* double mutant is presented here.

ant-4 ail6-2 flowers consist primarily of small green organs; they lack petals and only rarely produce some stamen-like organs (Fig. 1, M–O; Table I). The outermost organs of *ant-4 ail6-2* flowers resemble sepals in their overall shape and epidermal cell characteristics (Fig. 2, A–D). Other organs present in *ant-4 ail6-2* flowers include filaments, filaments that are swollen or expanded at their distal end (Fig. 2A; Table I), and organs resembling unfused carpel valves (Fig. 2, A, E, and F). Stigmatic tissue is occasionally present on the margins of these valve-like organs (Fig. 2F), but they completely lack internal tissue normally present within carpels. *ant-4 ail6-2* flowers sometimes contain other flat green organs that bear little resemblance to any floral organ found in wild-type flowers (Table I). Short filaments sometimes arise in the very center of *ant-4 ail6-2* flowers (Fig. 2B).

Defects in the development of *ant ail6* flowers are apparent at early stages. The floral meristem dome is often flatter in the double mutant (Figs. 2J and 3D) and/or consists of fewer cells (Fig. 2I). Fewer floral organ primordia are initiated, and they do not arise in regular positions (Fig. 2, I, J, and L). In both wild-type and *ant-4* flowers, four sepal primordia arise in a cross pattern, each arising approximately 90° from the adjacent primordium, with one primordium located in the position adaxial to the inflorescence meristem (Fig. 2, G and H). In *ant-4 ail6-2* flowers, a variable number of sepal primordia initiate at random positions within the floral meristem periphery (Fig. 2, I and J). Similarly, more centrally arising floral organ primordia do not exhibit any regular phyllotaxy (Fig. 2, K and L).

AP3 and *AG* Expression Is Altered in *ant ail6* Flowers

Because of the loss of petal, stamen, and carpel identities in *ant-4 ail6-2* flowers, I examined the expression of two floral organ identity genes: the class B gene *AP3* and the class C gene *AG*. RNA gel blots showed that both genes are expressed at reduced levels in the double mutant (Fig. 3, A and G), while

Table I. *Organs present in ant-4 ail6-2 and ant-4 flowers at positions 1 to 10, 11 to 20, and 21 to 30 on the inflorescence*

Organ counts were performed on four plants for each genotype.

Organ Type	*ant-4 ail6-2*			Organ Type	*ant-4*		
	1 to 10	11 to 20	21 to 30		1 to 10	11 to 20	21 to 30
Sepal	4.3	4.0	4.0	Sepal	3.85	3.73	3.85
Flat white	0.0	0.0	0.02	Petal	3.33	2.05	1.3
Filament	1.1	0.95	0.8	Filament	0.18	0.15	0.20
Swollen filament	1.8	0.2	0.1				
Stamen like	0.5	0.5	0.3	Stamen	4.88	4.33	4.25
Flat green	0.5	1.7	0.5				
Valve like	2.0	1.7	2.22	Carpel	2.0	2.0	2.0
Total	10.2	8.9	7.8	Total	14.2	12.3	11.6

in situ hybridization revealed that the spatial expression patterns are altered. In a stage 3 wild-type flower, *AP3* is expressed in cells adjacent to the sepal primordia that will give rise to the second and third whorls of the flower but not in the centermost cells of the floral meristem (Fig. 3B). Fewer cells in *ant-4 ail6-2* stage 3 flowers express *AP3* as compared with the wild type (Fig. 3, C and D). In addition, the central domain of non-*AP3*-expressing cells appears to be enlarged in *ant-4 ail6-2* double mutants (Fig. 3, C and D). Later in floral development, *AP3* is expressed in developing petals and stamens (Fig. 3E). In older *ant-4 ail6-2*

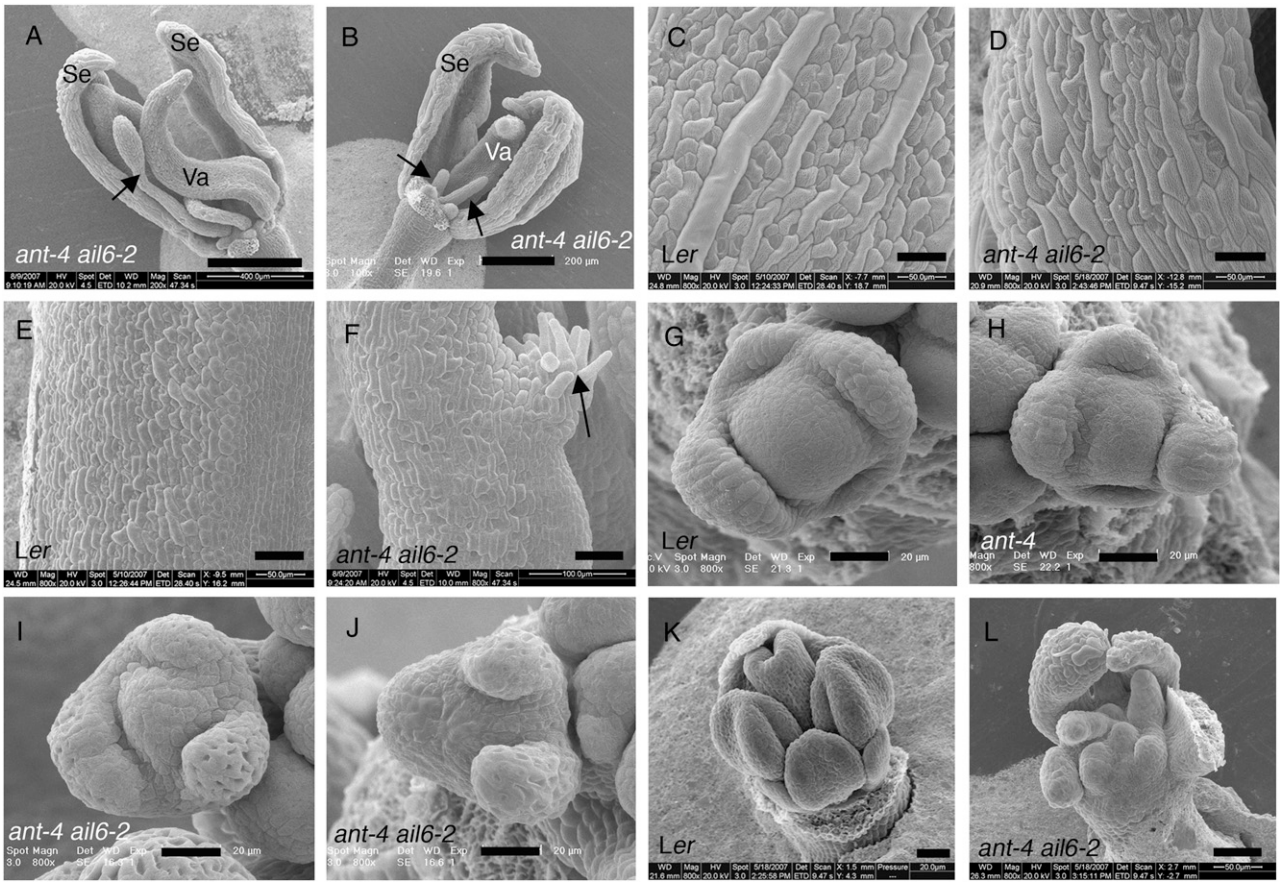

Figure 2. *ant-4 ail6-2* plants have defects in flower development. A, Mature *ant-4 ail6-2* flower with sepals (Se), unfused carpel valve-like structures (Va), and a stamen-like organ (arrow). B, Mature *ant-4 ail6-2* flower in which two short filaments (arrows) occupy the center of the flower. C, Abaxial surface of L*er* sepal. D, Abaxial surface of *ant-4 ail6-2* sepal. E, Epidermal surface of L*er* carpel valve. F, Epidermal surface of *ant-4 ail6-2* valve-like organ. An arrow points to stigmatic papillae present on the margin of the organ. G, Stage 4 L*er* flower. H, Stage 4 *ant-4* flower. I and J, Stage 4 *ant-4 ail6-2* flowers showing altered patterns of sepal initiation. K, Stage 10 L*er* flower in which three sepals have been dissected away. L, *ant-4 ail6-2* flower in which inner organ primordia have arisen in random positions. Bars = 400 μm in A, 200 μm in B, 50 μm in C to F and L, and 20 μm in G to K.

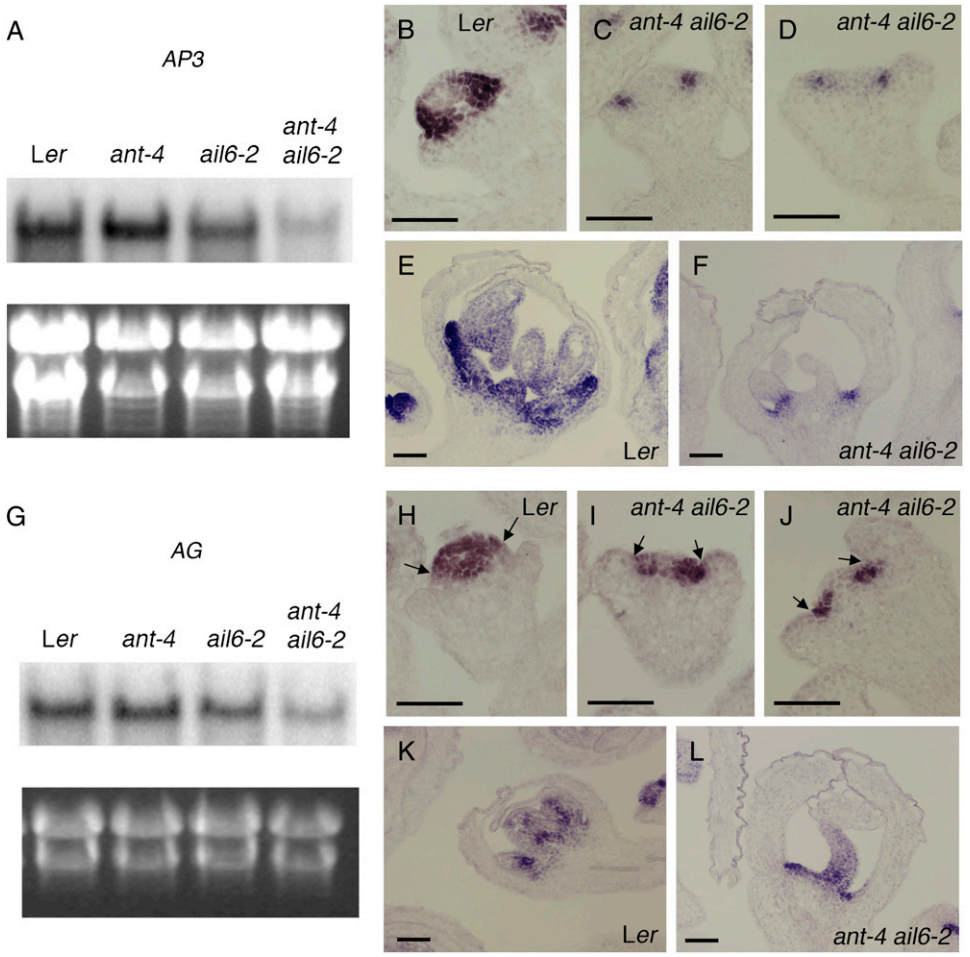

Figure 3. The expression patterns of *AP3* and *AG* are altered in *ant-4 ail6-2* flowers. A, RNA gel blot of *AP3* mRNA in L*er*, *ant-4*, *ail6-2*, and *ant-4 ail6-2* inflorescences. Ethidium bromide staining of ribosomal RNA is shown below the gel blot. B, *AP3* expression in stage 3 L*er* flower. C and D, *AP3* is expressed in fewer cells of stage 3 *ant-4 ail6-2* flowers. E, *AP3* expression in stage 10 L*er* flower. F, *AP3* mRNA was detected at the base of some floral organs in this *ant-4 ail6-2* flower. G, RNA gel blot of *AG* mRNA in L*er*, *ant-4*, *ail6-2*, and *ant-4 ail6-2* inflorescences. Ethidium bromide staining of ribosomal RNA is shown below the gel blot. H, *AG* expression in stage 3 L*er* flower. Arrows point to the outer boundary of *AG* expression. I and J, *AG* expression in stage 3 (I) and stage 4 (J) *ant-4 ail6-2* flowers. Arrows point to the outer boundary of *AG* expression. *AG* mRNA is not detected in the very central cells of the floral meristem. K, *AG* expression in stage 7 L*er* flower. L, *AG* expression is detected in some organs of older *ant-4 ail6-2* flowers. Bars = 50 μm in B to F and H to L. [See online article for color version of this figure.]

flowers, *AP3* expression is only observed in a few cells at the adaxial base of the outer whorl organs and/or at the base of more inwardly arising organs (Fig. 3F).

In stage 3 wild-type flowers, *AG* is expressed in cells of the floral meristem that will develop into the third and fourth whorls of the flower (Fig. 3H). In stage 3 and 4 *ant-4 ail6-2* flowers, *AG* mRNA is reduced and/or absent in the centermost cells of the floral meristem (Fig. 3, I and J). In addition, *AG* expression in the floral meristem directly abuts the sepal primordia in contrast to wild-type flowers, in which cells adjacent to the sepals do not express *AG* (Fig. 3, H–J). The extension of *AG* expression toward the sepals in *ant ail6* flowers is consistent with earlier work showing that *ANT* can act as a second whorl repressor of *AG* (Krizek et al., 2000). Ectopic *AG* expression in second whorl cells of *ant-4 ail6-2* flowers may be partly responsible for the decreased proliferation of these cells. In older wild-type flowers, *AG* is expressed in developing stamens and carpels (Fig. 3K). In *ant-4 ail6-2* flowers, *AG* expression is observed in interior organs with valve-like appearances (Fig. 3L).

To determine if the absence of *AG* mRNA in the center of *ant-4 ail6-2* floral meristems might be due to reduced expression of its activators, I examined *LFY* and *WUS* expression in the double mutant. *LFY* mRNA was detected in incipient floral primordia and throughout stage 1 and 2 flowers in both wild-type and *ant ail6* flowers (Fig. 4, A–D). Although the signal appeared to be weaker in some *ant ail6* flowers, no obvious difference in *LFY* mRNA levels could be detected by semiquantitative reverse transcription (RT)-PCR (Supplemental Fig. S2). In wild-type stage 3 flowers, *LFY* expression is strong and uniform throughout the sepal primordia and floral meristem (Fig. 4C). However, in stage 3 *ant-4 ail6-2* flowers, *LFY* expression is found to be patchy (Fig. 4D). In contrast to *LFY* expression, *WUS* expression is increased in young *ant-4 ail6-2* flowers (Fig. 4, E and F). In addition, *WUS* expression is detected in a broader domain in the double mutant that includes L1, L2, and L3 cells (Fig. 4, G and H).

ANT and *AIL6* Regulate Floral Meristem Proliferation

As *AG* activity is required to down-regulate *WUS* expression but is missing from the central region of stage 3 *ant-4 ail6-2* flowers, *WUS* expression was examined in older *ant-4 ail6-2* flowers. Persistent *WUS* expression was sometimes observed in the cen-

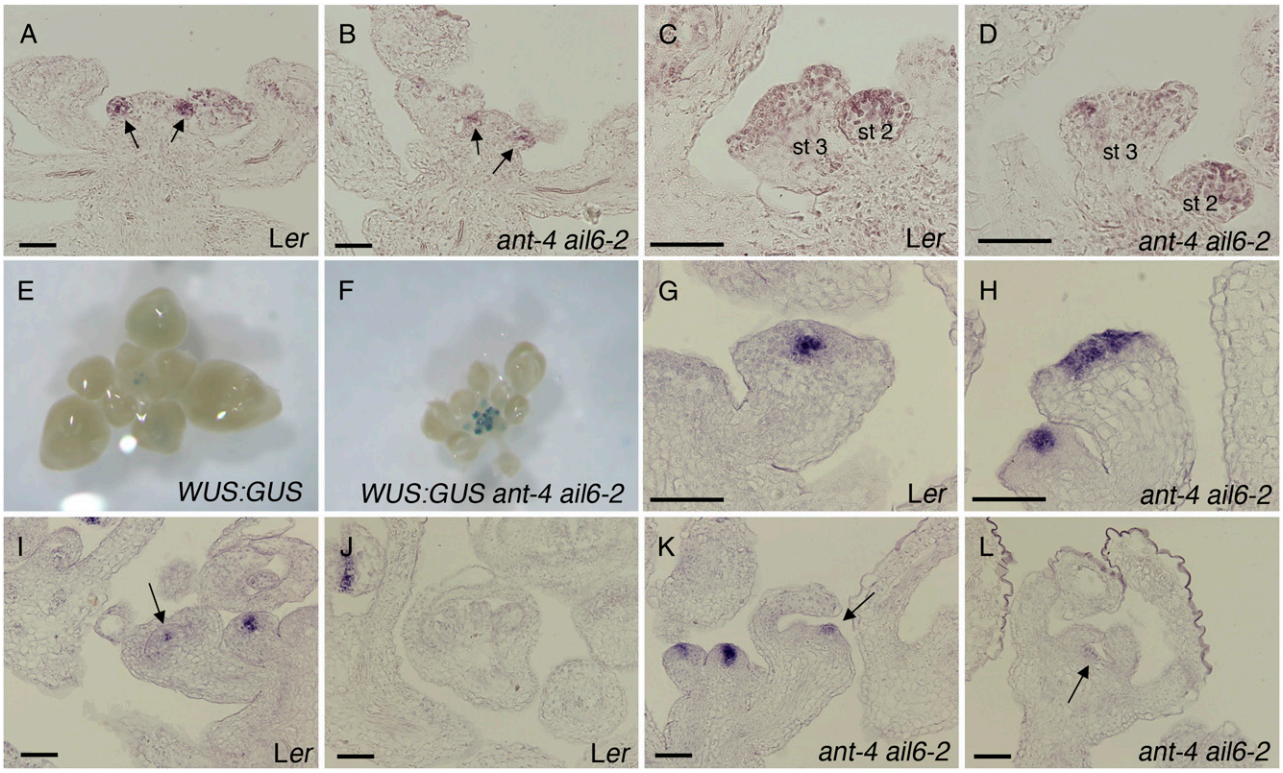

Figure 4. The expression patterns of *LFY* and *WUS* are altered in *ant-4 ail6-2* flowers. A, *LFY* expression in a L*er* inflorescence. Arrows point to incipient floral primordia (right) and a stage 1 floral meristem (left). B, *LFY* expression in an *ant-4 ail6-2* inflorescence. Arrows point to incipient floral primordia (left) and a stage 1 floral meristem (right). C, *LFY* expression in stage 2 (st 2) and stage 3 (st 3) L*er* flowers. D, *LFY* expression in stage 2 and stage 3 *ant-4 ail6-2* flowers. *LFY* expression is not as uniform in stage 3 *ant-4 ail6-2* flowers compared with L*er*. E, *WUS:GUS* inflorescence showing GUS staining in the very center of the inflorescence. F, *WUS:GUS ant-4 ail6-2* inflorescence showing strong GUS staining in young flowers. G, *WUS* expression in the center region of a stage 3 wild-type flower. H, *WUS* mRNA is detected in a broader domain in this stage 3 *ant-4 ail6-2* flower. I, The arrow points to *WUS* expression in a stage 5 wild-type flower. J, *WUS* is not expressed in a stage 7 wild-type flower. K and L, The arrows point to *WUS* expression in older *ant-4 ail6-2* flowers. Bars = 50 μm in A to D and G to L.

tral region of *ant-4 ail6-2* flowers at stages after *WUS* expression had disappeared from wild-type flowers (Fig. 4, I–L). While persistent expression of *WUS* in *ag* flowers results in floral meristem indeterminacy (Lenhard et al., 2001; Lohmann et al., 2001), such indeterminacy was never observed in *ant-4 ail6-2* flowers, suggesting that *ANT* and *AIL6* activities are required for floral meristem proliferation.

This possibility was investigated by constructing the *ag-1 ant-4 ail6-2* triple mutant. *ag-1 ant-4 ail6-2* flowers are determinate and consist primarily of sepals with a few petal-like organs (Fig. 5, A and B). *ag-1 ant-4 ail6-2* flowers typically produce just a few more floral organs than *ant-4 ail6-2* flowers (Fig. 5C). In a few *ag-1 ant-4 ail6-2* flowers, many more floral organs were produced, but these flowers were never indeterminate (Fig. 5D). Thus, *ANT* and *AIL6* are required for the continued proliferation of the floral meristem in *ag* mutants. The partial restoration of petal identity in *ag-1 ant-4 ail6-2* flowers and the increased number of floral organs could be due to increased proliferation of second whorl cells in the absence of *AG*.

ANT and *AIL6* Promote Growth of All Shoot-Derived Organs

ant-4 ail6-2 plants also exhibit defects during vegetative development. The plants are reduced in height, with a bushier appearance due to the outgrowth of additional axillary inflorescences from rosette and cauline leaves (Fig. 6A; Table II). In addition, accessory meristems in cauline leaf axils exhibit enhanced outgrowth in *ant-4 ail6-2* plants (Fig. 6B). Both leaves and flowers produced by *ant-4 ail6-2* plants are reduced in size compared with those from *ant-4* and wild-type plants (Fig. 6, C–F). Rosette leaves of the double mutant plants are thinner than those from *ant-4* and wild-type plants (Fig. 6, C–E), with alterations in leaf vein architecture (Supplemental Fig. S3). *ant-4 ail6-2* leaves show more severe defects in vein density and complexity than those previously reported for *ant* single mutants (Supplemental Fig. S3, B and C; Kang et al., 2007).

Epidermal cells of rosette leaves and sepals were similar in size in both the wild type and *ant-4 ail6-2*,

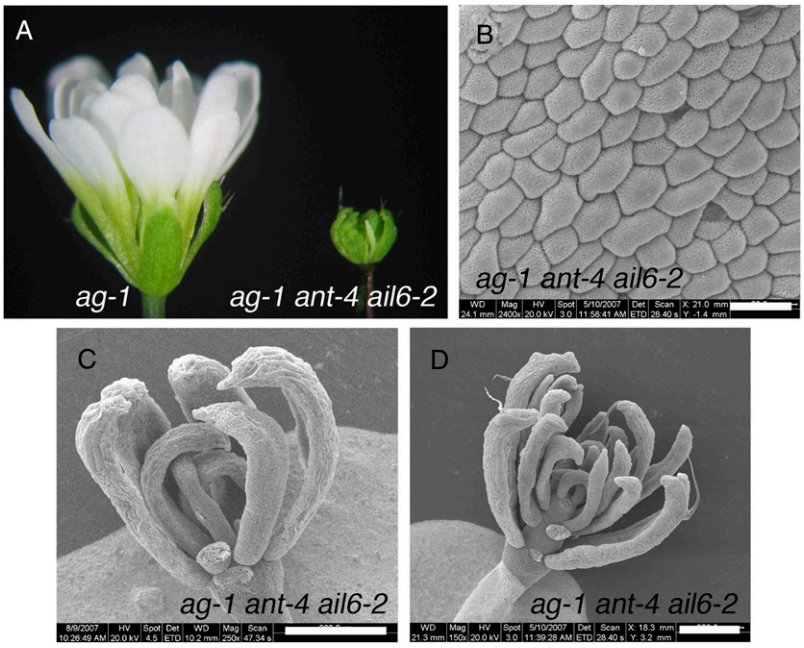

Figure 5. *ag-1 ant-4 ail6-2* flowers are determinate. A, *ag-1* (left) and *ag-1 ant-4 ail6-2* (right) flowers. B, Scanning electron micrograph of the epidermal cells of a second whorl petal-like organ from an *ag-1 ant-4 ail6-2* flower. C, Scanning electron micrograph of a typical *ag-1 ant-4 ail6-2* flower. D, Scanning electron micrograph of an *ag-1 ant-4 ail6-2* flower that produces a greater number of organs but is still determinate. Bars = 20 μm in B and 300 μm in C and D. [See online article for color version of this figure.]

suggesting that the reduced size of these organs results primarily from fewer cells (Figs. 2, C and D, and 6, G and H). Epidermal peels of stems at positions midway along the primary inflorescence revealed similar cell lengths in wild-type and *ant-4 ail6-2* plants (Fig. 6, I and J). However, cells making up the internodes between successive flowers of *ant-4 ail6-2* plants are dramatically reduced in length in *ant-4 ail6-2* plants as compared with wild-type plants (Fig. 6, K and L). Thus, the reduced height of *ant-4 ail6-2* plants appears to arise primarily from reduced internode length.

ANT and *AIL6* Are Required for Continued Shoot Apical Meristem Function

Initially, the inflorescence meristems of *ant-4 ail6-2* plants have a dome appearance similar to the wild type (Fig. 7, A and B). However, as reproductive development proceeds, *ant-4 ail6-2* inflorescence meristems become increasingly sloped, with flowers initiating at positions farther down the sides of the meristem (Fig. 7, C and D). Floral initiation eventually ceases in *ant-4 ail6-2* plants, with the inflorescence meristem and surrounding floral primordia aborting growth. While the total number of flowers initiated by *ant-4 ail6-2* inflorescence meristems prior to termination is similar to the number produced by wild-type plants prior to senescence (36.2 $\pm$ 3.0 in the wild type versus 33.3 $\pm$ 4.0 in *ant-4 ail6-2*), it is less than that produced by sterile mutants such as *ant-4* (44.4 $\pm$ 8.5).

To gain insight into the basis for these defects in meristem function, I examined the expression of two important regulators of shoot apical meristem activity, *WUS* and *CLAVATA3* (*CLV3*). *WUS* expression is confined to a small group of underlying cells in the shoot apical meristem referred to as the organizing center (Fig. 7G), while *CLV3* is expressed in the overlying stem cells (Fig. 7E; Mayer et al., 1998; Fletcher et al., 1999). In *ant-4 ail6-2* plants, *CLV3* expression extends deeper into the inflorescence meristem than in the wild type (Fig. 7F), while *WUS* expression moves up into L1 and L2 cells within the center of the meristem (Fig. 7H). These changes and the partial overlap of the *WUS* and *CLV3* expression domains suggest that cells within *ant-4 ail6-2* inflorescence meristems have altered and/or mixed identities, since they express markers for both stem cell and organizing center fate.

ant ail6 Flowers Display Altered Expression of the Auxin-Responsive Reporter *AGH3-2:GUS*

Because several of the defects observed in *ant-4 ail6-2* plants are reminiscent of mutants disrupted in auxin physiology, I examined auxin responses in *ant-4 ail6-2* inflorescences using the auxin reporter *AGH3-2:GUS*. This reporter contains approximately 1.1 kb of 5′ sequence from the Arabidopsis *GH3-2* gene (At4g37390; G. Hagen, personal communication). The *AGH3-2:GUS* reporter shows a similar pattern of expression in inflorescences and flowers as *DR5(rev):GFP*, with expression in incipient floral primordia (Fig. 8A) and the tips of developing floral organs (Fig. 8, E, G, and I; Benkova et al., 2003; Heisler et al., 2005; Smith et al., 2006). Many *AGH3-2:GUS ant-4 ail6-2* inflorescences showed GUS activity in incipient floral primordia similar to that observed in *AGH3-2:GUS* (Fig. 8B). However, in some *AGH3-2:GUS ant-4 ail6-2* inflorescences, GUS staining was observed in a broader domain that extended deeper into the inflorescence meristem (Fig. 8, C and D). Differences in the expression of *AGH3-2:GUS* in the double mutant were more dramatic in flowers. In *AGH3-2:GUS ant-4 ail6-2* flow-

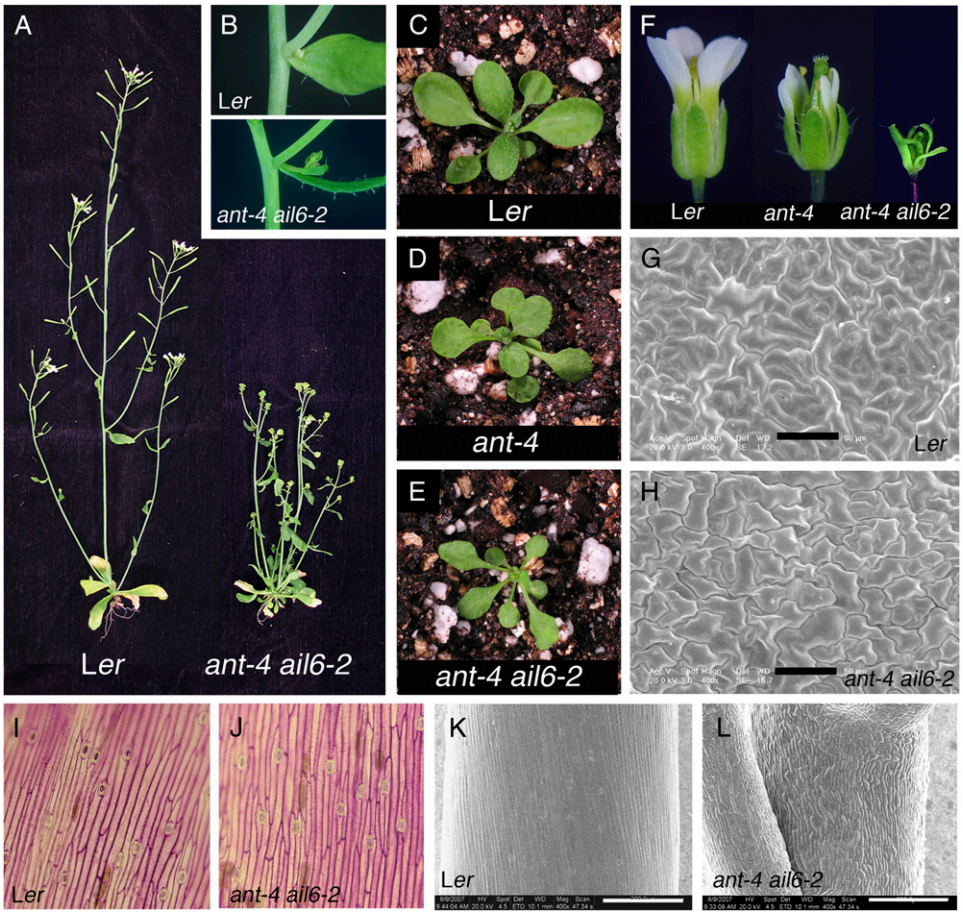

Figure 6. *ant-4 ail6-2* plants are reduced in height and produce smaller leaves and flowers. A, Size comparison of L*er* and *ant-4 ail6-2* plants. B, Outgrowth of accessory meristems in the leaf axil of *ant-4 ail6-2* but not L*er* plants. C to E, Rosettes of L*er* (C), *ant-4* (D), and *ant-4 ail6-2* (E) plants. F, Size comparison of L*er*, *ant-4*, and *ant-4 ail6-2* flowers. G, Scanning electron micrograph of L*er* rosette leaf. H, Scanning electron micrograph of *ant-4 ail6-2* rosette leaf shows epidermal cells similar in size to those of L*er*. I, Epidermal peel from middle region of L*er* stem. J, Epidermal peel from middle region of *ant-4 ail6-2* stem. K, Scanning electron micrograph of upper region of L*er* stem. L, Scanning electron micrograph of upper region of *ant-4 ail6-2* stem. Bars = 50 μm in G and H and 200 μm in K and L.

ers, GUS activity was not restricted to the tips of developing organs (Fig. 8, F, H, and J). GUS activity was often highest in the central provascular tissue of developing floral organs (Fig. 8H). These differences suggest that auxin responses, distribution, and/or levels are altered in *ant-4 ail6-2* flowers. *ant-4 ail6-2* plants are responsive to exogenous auxin, as increased GUS expression was observed in *AGH3-2:GUS ant-4 ail6-2* inflorescences treated with 50 μM indole-3-acetic acid (IAA; Fig. 8, K and L).

Auxin Transport Is Necessary for *ANT* Expression in Incipient Flowers

As *ANT* and *AIL6* expression in incipient floral primordia (Nole-Wilson et al., 2005) correlates with auxin accumulation in these cells (Reinhardt et al., 2003; Heisler et al., 2005; Barbier de Reuille et al., 2006; Smith et al., 2006), I investigated whether auxin might play a role in transcriptional regulation of *ANT*. No differences in *ANT* mRNA levels were detected in L*er* inflorescences collected 24 h after treatment with 50 μM IAA or 50 μM 2,4-dichlorophenoxyacetic acid as compared with a mock solution (Supplemental Fig. S4, A and B). In addition, no change in the spatial pattern of *ANT* expression, as assessed using an *ANT:GUS* reporter line, was observed (Supplemental Fig. S4, C–F). The promoter fragment used in this construct is sufficient to complement *ant-4* when fused to the *ANT* coding sequence (Supplemental Fig. S5).

Because auxin may be necessary but not sufficient for *ANT* regulation, I treated inflorescences with the auxin transport inhibitor NPA. No difference in *ANT* mRNA levels was detected in L*er* inflorescences treated with 100 μM NPA for 24 h as compared with mock-treated tissue (Fig. 9, A and B). However, *ANT* expression was reduced in incipient floral primordia and stage 1 and 2 flowers of NPA-treated *ANT:GUS* inflorescences (Fig. 9, C and D). No obvious changes in *ANT* expression were observed in older flowers. Sim-

Table II. *Plant heights and number of axillary inflorescences*

Plant height and number of axillary inflorescences were determined for 12 plants of each genotype.

Plant	Height	No. of Axillary Inflorescences (Rosette)	No. of Axillary Inflorescences (Cauline)
	cm		
L*er*	21.8 ± 1.37	0.50 ± 0.80	2.50 ± 0.52
ant-4	20.0 ± 2.74	1.08 ± 1.00	2.67 ± 0.65
ant-4 ail6-2	11.6 ± 2.70	3.42 ± 1.31	3.33 ± 1.07

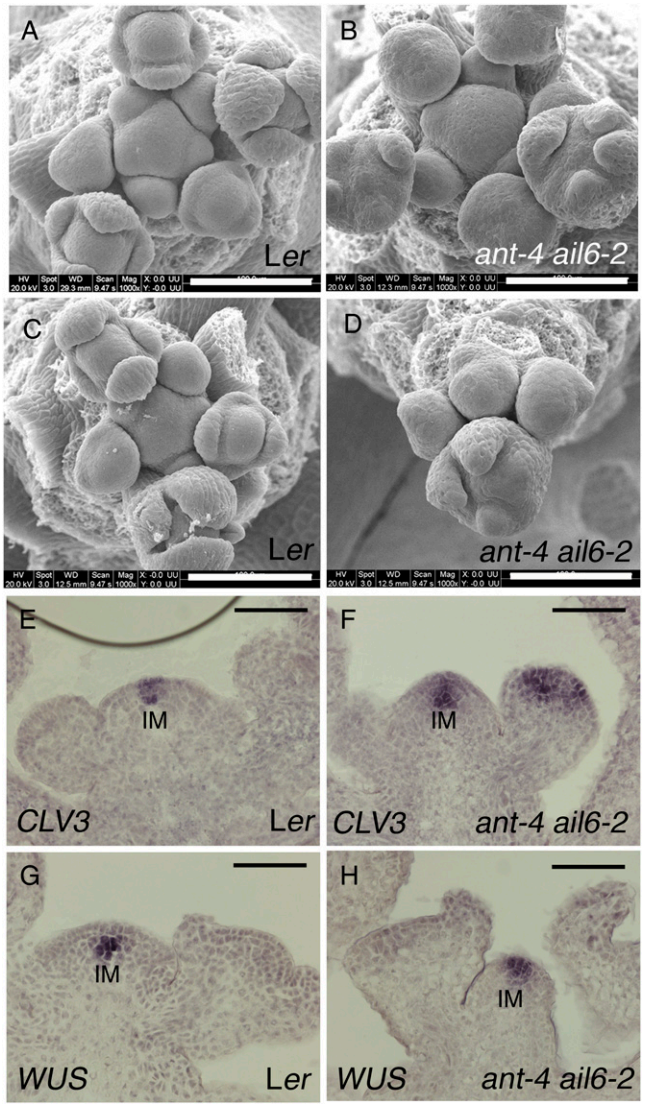

Figure 7. Inflorescence meristems (IM) of *ant-4 ail6-2* plants exhibit growth arrest and show altered expression of meristem regulators. A, Scanning electron micrograph of the apex of a 22-d-old L*er* plant. B, Scanning electron micrograph of the apex of a 22-d-old *ant-4 ail6-2* plant. C, Scanning electron micrograph of the apex of a 30-d-old L*er* plant. D, Scanning electron micrograph of the apex of a 30-d-old *ant-4 ail6-2* plant. E, *CLV3* expression in a L*er* inflorescence. F, *CLV3* mRNA is detected in a broader domain corresponding to L1, L2, and L3 cells within the inflorescence meristem of *ant-4 ail6-2* plants. G, *WUS* expression in a L*er* inflorescence. H, *WUS* mRNA is detected in the uppermost cells of the inflorescence meristem in *ant-4 ail6-2* plants. Bars = 100 μm in A to D and 50 μm in E to H. [See online article for color version of this figure.]

ilar results were obtained by in situ hybridization examining *ANT* mRNA in L*er* inflorescences treated with NPA (Fig. 9, E and F). Thus, auxin transport within the inflorescence meristem is necessary for high levels of *ANT* expression in the very earliest stages of flower development but not for *ANT* expression in older flowers. The observed reduction in *ANT* expression is observed prior to morphological changes in lateral organ initiation that occur as a consequence of NPA treatment (Fig. 9, G and H; Okada et al., 1991; Reinhardt et al., 2000). The inability to detect changes in *ANT* mRNA levels in the RT-PCR experiment likely results from the very small contribution of cells from early floral primordia to the entire inflorescence harvested for the RT-PCR experiment.

DISCUSSION

ANT and *AIL6* Regulate Flower Development

ANT and *AIL6* regulate several aspects of flower development, including floral meristem and organ growth, organ positioning within the floral meristem, and specification of floral organ identity. *ant ail6* flowers contain fewer organs per flower than the wild type, as well as organs such as filaments and flat green organs that are not normally found in wild-type flowers. Thus, the absence of petals and stamens likely results from defects in both organ initiation and organ identity specification. Defects in organ initiation may be a consequence of insufficient cells within the floral meristem, while defects in organ identity specification likely result from altered expression of the floral organ identity genes *AP3* and *AG*.

Similar *LFY* expression in *ant ail6* and wild-type flowers of stages 1 and 2 suggests that ANT and AIL6 promote *AP3* and *AG* expression through a LFY-independent pathway (Fig. 10). However, nonuniform *LFY* expression in stage 3 *ant ail6* flowers suggests that *ANT* and *AIL6* may also promote floral organ identity gene expression through the maintenance of *LFY* expression (Fig. 10). The expanded *WUS* expression domain in *ant ail6* flowers suggests that *WUS* is not limiting for *AG* activation. I examined *LFY*, *AP3*, and *AG* regulatory regions (Blazquez et al., 1997; Hill et al., 1998; Tilly et al., 1998; Busch et al., 1999; Deyholos and Sieburth, 2000) for the presence of potential ANT-binding sites (Nole-Wilson and Krizek, 2000). One such site with two mismatches compared with the consensus site was identified in the *LFY* promoter (−1,380 to −1,394 relative to the start codon), while no sequences with three or fewer mismatches were present within 800 bp of *AP3* 5′ sequence. This suggests that the regulation of *AP3* by ANT and AIL6 may be indirect.

The presence of five potential ANT-binding sites, each containing three mismatches, within the *AG* second intron suggests that ANT and AIL6 may be direct regulators of *AG* expression. Previous work has shown that *ANT* acts as a repressor of *AG* expression, preventing precocious *AG* expression in flowers (Liu et al., 2000) and acting redundantly with *AP2* in repression of *AG* in the second whorl (Krizek et al., 2000). The data presented here show that *ANT* and *AIL6* act redundantly to negatively regulate *AG* expression in second whorl cells and to positively regulate *AG* expression in the centermost cells of the floral

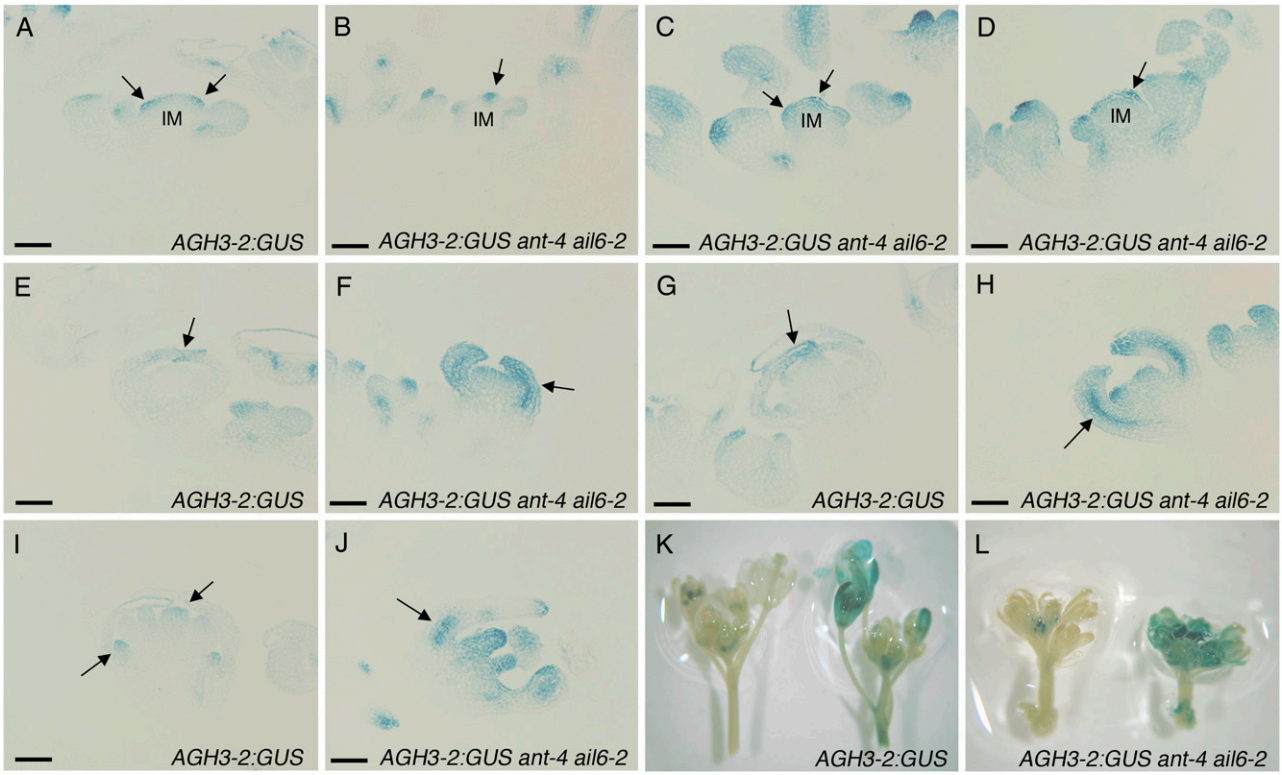

Figure 8. Altered expression of the *AGH3-2*:*GUS* auxin-responsive reporter in *ant-4 ail6-2* inflorescences. A, GUS-stained *AGH3-2*:*GUS* inflorescence. Arrows point to incipient floral primordia. B, GUS-stained *AGH3-2*:*GUS ant-4 ail6-2* inflorescence. The arrow points to an incipient floral primordium. C and D, GUS-stained *AGH3-2*:*GUS ant-4 ail6-2* inflorescences with broader *AGH3-2*:*GUS* activity throughout the inflorescence meristem (IM). Arrows point to incipient floral primordia. E, *AGH3-2*:*GUS* stage 5 flower showing GUS staining at the tips of the developing sepals. F, *AGH3-2*:*GUS ant-4 ail6-2* flower with GUS staining throughout the developing sepals. G, *AGH3-2*:*GUS* stage 7 flower showing GUS staining at the tips of the developing sepals (arrow). H, *AGH3-2*:*GUS ant-4 ail6-2* flower with GUS staining throughout the developing sepals, with strongest staining in the provascular cells (arrow). I, *AGH3-2*:*GUS* stage 10 flower showing GUS staining at the tips of the developing floral organs (arrows). J, *AGH3-2*:*GUS ant-4 ail6-2* flower with GUS staining at the base of the sepals (arrow) and throughout other organs. K, GUS-stained mock-treated (left) and IAA-treated (right) *AGH3-2*:*GUS* inflorescences. L, GUS-stained mock-treated (left) and IAA-treated (right) *AGH3-2*:*GUS ant-4 ail6-2* inflorescences. Bars = 50 μm in A to J.

meristem (Fig. 10). Thus, the role of ANT and AIL6 in *AG* regulation appears to be context dependent and likely involves different coregulators.

ANT and *AIL6* Are Required for the Proliferation and Maintenance of a Meristematic Cell Fate

In *ag* mutants, persistent *WUS* expression in stage 6 and older flowers results in floral indeterminacy (Lenhard et al., 2001; Lohmann et al., 2001). Additional regulators of floral determinacy have recently been identified and include *perianthia* (*pan*) and three enhancers of *crabs claw* (*crc*): *rebelote* (*rbl*), *squint* (*sqn*), and *ultrapetala1* (*ult1*; Prunet et al., 2008; Das et al., 2009; Maier et al., 2009). In *crc sqn* and *crc ult* double mutants and in a dominant-negative *pan* allele, *AG* expression is reduced in the very center of stage 3 flowers, similar to what is seen in *ant ail6* flowers (Prunet et al., 2008; Das et al., 2009). It has been proposed that this region corresponds to an inner fourth whorl subdomain in which meristematic potential can be maintained (Prunet et al., 2008). *SQN*, *ULT1*, and *PAN* promote *AG* expression in this subdomain, consequently resulting in *WUS* down-regulation and termination of stem cell fate (Prunet et al., 2008; Das et al., 2009; Maier et al., 2009).

ANT and *AIL6* also appear to regulate *AG* expression in this inner fourth whorl domain, but unlike other genetic backgrounds in which persistent *WUS* expression results in indeterminacy, *ant ail6* flowers are determinate. Furthermore, I have found that *ANT* and *AIL6* activity is required for the indeterminacy of *ag* flowers. Thus, *WUS* itself is not sufficient for floral meristem indeterminacy but requires factors such as *ANT* and *AIL6* that promote continued proliferation of stem cells. In the absence of *ANT* and *AIL6*, these cells do not proliferate to maintain a stem cell pool from which organ primordia can be initiated.

The eventual termination of *ant ail6* inflorescence meristems also supports a role for *ANT* and *AIL6* in

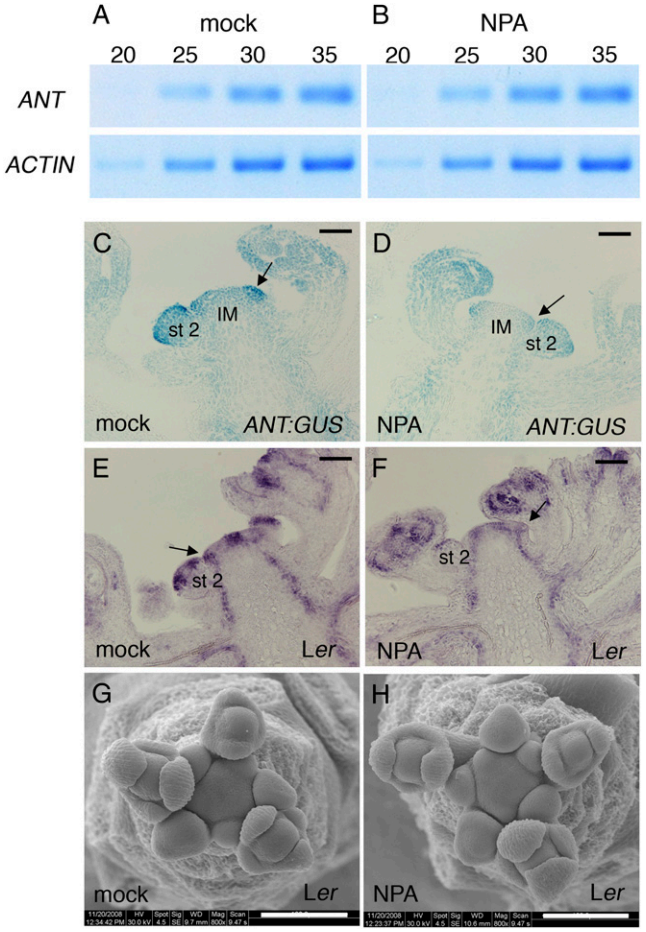

Figure 9. *ANT* expression is responsive to NPA treatment. A and B, Semiquantitative RT-PCR of *ANT* and *ACTIN* (internal control) mRNA levels in inflorescences 24 h after mock (A) or NPA (B) treatment. C and D, *ANT*:*GUS* inflorescence stained for GUS 24 h after mock (C) or NPA (D) treatment. GUS staining is weaker in the incipient floral primordium (arrow) and stage 2 (st 2) flower of the NPA-treated inflorescence compared with the mock-treated inflorescence. E and F, *ANT* expression in L*er* inflorescences fixed 24 h after mock (E) or NPA (F) treatment. *ANT* mRNA levels are reduced in the incipient floral primordium (arrow) and stage 2 flower of the NPA-treated inflorescence compared with the mock-treated inflorescence. G and H, Scanning electron micrographs of L*er* inflorescences fixed 24 h after mock (G) or NPA (H) treatment. IM, Inflorescence meristem. Bars = 50 μm in C to F and 100 μm in G and H.

stem cell proliferation. The basis for shoot apical meristem termination in *ant ail6* plants is not clear. While the width of the inflorescence meristem gets progressively smaller during development, it does not appear that all meristematic cells are consumed in the process of lateral organ initiation. Rather, there appears to be an arrest of the shoot apex with the cessation of new floral initiation and growth abortion of young primordia. The expression patterns of *CLV3* and *WUS* are altered in *ant ail6* inflorescence meristems, with both genes expressed in a broader domain and some cells within the central part of the meristem expressing both *CLV3* and *WUS*. The broader expression domains of these central zone markers might indicate a loss of peripheral zone identity and consequently an inability to initiate new primordia.

ANT May Act Downstream of Auxin

Roles for ANT and AIL6 in auxin regulation of flower development are suggested by the apparent overlap between transient auxin maxima within the inflorescence meristem (Reinhardt et al., 2003; Heisler et al., 2005; Barbier de Reuille et al., 2006; Smith et al., 2006) and the expression of *ANT* and *AIL6* within incipient floral primordia (Nole-Wilson et al., 2005). In addition, the spatial expression pattern of *ANT* is altered in *pin1* mutants, with *ANT* mRNA detected in a ring around the periphery of the naked shoot apex rather than in distinct groups of cells (Vernoux et al., 2000). This change in *ANT* expression could be a direct consequence of altered auxin accumulation patterns in *pin1* mutants or an indirect consequence related to the inability of *pin1* mutants to initiate flowers. Here, I show that *ANT* expression is reduced in incipient floral primordia and young flowers 24 h after NPA treatment. This change in expression occurs prior to any morphological change in the meristem, suggesting that auxin transport plays a relatively direct role in *ANT* regulation.

ant ail6 mutants are dwarfed, display altered organ growth, and have reduced amounts of vascular tissue, phenotypes similar to mutants defective in auxin physiology. Treatment of *ant ail6* inflorescences with exogenous auxin showed that these plants could re-

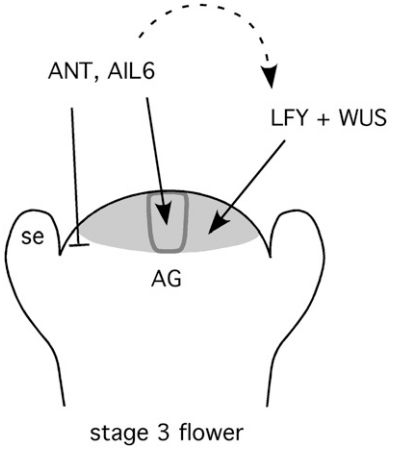

Figure 10. Model for *AG* regulation by ANT and AIL6. In a stage 3 flower, *AG* expression in the floral meristem (gray) is promoted by the combined action of LFY and WUS. ANT and AIL6 promote *AG* expression in the centermost part of the floral meristem via a pathway that is likely to be independent of the LFY-WUS pathway. This centermost region is outlined in dark gray. ANT and AIL6 may also indirectly promote *AG* expression via maintenance of *LFY* expression (dotted arrow). ANT and AIL6 repress *AG* expression in second whorl cells (bar). se, Sepal.

spond to auxin, suggesting that at least some primary auxin responses mediated by ARFs are functional in these plants. If ANT and AIL6 do function in auxin signaling, presumably they do so downstream of ARFs. Two potential AuxREs are present within the *ANT* promoter at positions −1,083 to −1,078 and −2,525 to −2,520 relative to the start codon. No sequences with similarity to AuxRE were identified in *AIL6* regulatory regions. Altered expression of the auxin-responsive reporter *AGH3-2:GUS* in *ant ail6* flowers may indicate defects in some auxin responses or alternatively that auxin levels and/or distribution are altered in *ant ail6* inflorescences. Future experiments need to be conducted to investigate these different possibilities. A role for ANT and AIL6 in mediating auxin distribution would not preclude a possible role for these proteins in signaling downstream of auxin. Feedback between the auxin distribution system and auxin signaling pathways allows the plant to coordinate developmental processes and respond to changing environmental conditions (Leyser, 2006; Benjamins and Scheres, 2008). PLT proteins in the root are thought to regulate developmental patterning in response to auxin as well as auxin distribution (Blilou et al., 2005; Benjamins and Scheres, 2008).

Parallels between *AIL/PLT* Function in Roots and Shoots

Members of the *AIL/PLT* gene family play important and somewhat similar roles in roots and shoots. While *plt1* and *plt2* single mutants show subtle root defects, *plt1 plt2* double mutants exhibit reduced root growth, altered cellular patterning in the root tip, and termination of the root apical meristem by 6 to 8 d after germination (Aida et al., 2004). Thus, in both roots and shoots, *AIL/PLT* genes act redundantly to regulate organ growth, developmental patterning, and meristem maintenance. *AIL6/PLT3* also acts redundantly with *PLT1* and *PLT2* in the root (Galinha et al., 2007), demonstrating that *AIL6* is an important regulator of both root and shoot development.

PLT function has been proposed to promote root growth and patterning downstream of auxin. The highest accumulation of PLT1, PLT2, AIL6/PLT3, and BBM proteins in the root occurs in the stem cell niche, which corresponds to a stable auxin maximum (Galinha et al., 2007). *PLT1* and *PLT2* mRNA levels increase approximately 24 h after treatment of seedlings with auxin, and their expression is largely absent in embryos lacking functional copies of two ARFs (Aida et al., 2004). The work presented here suggests that ANT and AIL6 function downstream of auxin in flowers. Thus, members of the *AIL/PLT* gene family may represent components of a conserved mechanism by which auxin gradients are converted into growth and patterning outputs within both roots and shoots despite differences in the nature of the auxin maxima in roots and shoots.

MATERIALS AND METHODS

Plant Growth Conditions

Arabidopsis (*Arabidopsis thaliana*) plants were grown on a soil mixture of either Metro-Mix 360:perlite:vermiculite (5:1:1) or Miracle Gro Moisture Control Potting Mix:perlite:vermiculite (5:1:1) under continuous light or in 16-h days (100–150 μmol m^{-2} s^{-1}) at a temperature of 22°C.

PCR Genotyping

DNA was isolated from leaves and used in PCR for genotyping (Klimyuk et al., 1993). The *AIL6* T-DNA alleles were PCR genotyped using a pair of gene-specific primers and a T-DNA primer. *ant-4* contains a single T-to-A transversion that alters the donor splice site of the fourth intron (Nole-Wilson and Krizek, 2006). *ant-4* was genotyped by Tetra-primer ARMS-PCR using TPANT-1 (5′-GATGATCTTCTTCTCAGTTTATCTGCGA-3′), TPANT-2 (5′-TGAATCCATGAAGATTGAAGTGTGTACATA-3′), TPANT-3 (5′-GGACAATAGTTTCAAGAAGGAAGGTCAC-3′), and TPANT-4 (5′-CCAGTACTTGAGTGCAGCAAGATCATAT-3′; Ye et al., 2001). PCRs of 100 μL contained 100 pmol of TPANT-1 and TPANT-2 and 10 pmol of TPANT-3 and TPANT-4 and consisted of 35 cycles with the following conditions: 1 min at 95°C, 1 min at 55°C, and 1 min at 72°C followed by one cycle of 2 min at 72°C. The allele-specific PCR product for *ant-4* is 199 bp, while that for the wild type is 230 bp.

In Situ Hybridization

Inflorescences were fixed, embedded, sectioned, hybridized, and washed as described previously (Krizek, 1999). Digoxigenin-labeled antisense RNA probes (*AIL6*, *AP3*, *AG*, *LFY*, *WUS*, and *CLV3*) were synthesized as described previously (Yanofsky et al., 1990; Jack et al., 1992; Weigel et al., 1992; Mayer et al., 1998; Fletcher et al., 1999; Nole-Wilson et al., 2005).

Scanning Electron Microscopy

Tissue for scanning electron microscopy was fixed, dried, dissected, and coated as described previously (Krizek, 1999). Scanning electron microscopy analyses were performed on either a FEI XL30 ESEM or a FEI Quanta 200 ESEM apparatus.

RNA Isolation and Gel-Blot Analyses

Inflorescences (corresponding to all unopened floral buds) were homogenized in liquid nitrogen, and total RNA was isolated with hot phenol extraction buffer (Verwoerd et al., 1989). Total RNA (10 μg) was separated on a 0.66% formaldehyde, 1% agarose gel, transferred to a Nytran SuperCharge membrane, and hybridized with RNA probes. [^{32}P]UTP-labeled RNA probes were synthesized using the *AP3* and *AG* linearized plasmids described above for in situ hybridization. The blots were scanned on a Molecular Dynamics Storm 860 PhosphorImager.

Semiquantitative RT-PCR

Total RNA was treated for 4 to 6 h with RQ1 RNase-free DNase (Fisher Scientific) at 37°C. Approximately 5 μg of total RNA was reverse transcribed using the SuperScript III first-strand synthesis system (Invitrogen). PCR conditions were 40 cycles of 30 s at 92°C, 30 s at 50°C, and 2 min at 72°C and one cycle of 5 min at 72°C. Aliquots (5 μL) were removed at five-cycle intervals starting with cycle 20. Actin transcript levels confirmed that equivalent amounts of cDNA were used in the experiment.

Epidermal Peels, Plant Measurements, and Leaf Vascular Staining

The epidermis was removed from a midsection of the inflorescence stem of 5-week-old plants, placed on a drop of water on a glass slide, and stained briefly with toluidene blue. Plants used in height measurements and axillary inflorescence counts were germinated on plates and transplanted into soil at 7 d after germination. Plant height was measured and the number of axillary inflorescences from rosette and cauline leaves was counted when the plants

were 6 weeks old. Vascular tissue was examined by fixing the sixth leaf of 25-d-old plants overnight at room temperature in a 3:1 solution of ethanol:acetic acid. The leaves were mounted in 70% ethanol and photographed using a dissecting microscope with illumination from below.

GUS Staining

The GUS assays were performed as described previously (Krizek and Meyerowitz, 1996) except that the tissue was incubated in 2 mM 5-bromo-4-chloro-3-indolyl-β-glucuronic acid for 9 h (sectioned *ANT*:*GUS* and *AGH3-2*:*GUS*) or 22 h (whole mount *WUS*:*GUS* and *AGH3-2*:*GUS*) at 37°C. The tissue was either photographed as whole mounts or embedded in paraplast, sectioned, mounted on slides, and observed under bright-field illumination.

Auxin and NPA Treatment of Inflorescences

AGH3-2:*GUS* and *AGH3-2 ant-4 ail6-2* inflorescences were treated with 50 μM IAA (in 0.05% methanol and 0.01% Silwet L-77) or a mock solution (0.05% methanol and 0.01% Silwet L-77) using a paintbrush, harvested 6 h after treatment, and stained for GUS. L*er* and *ANT*:*GUS* inflorescences were painted with 50 μM IAA (in 0.05% methanol and 0.01% Silwet L-77) or a mock solution (0.05% methanol and 0.01% Silwet L-77) and harvested 24 h after treatment. Similar treatments were conducted with 50 μM 2,4-dichlorophenoxyacetic acid (in 0.05% ethanol and 0.01% Silwet L-77) or a mock solution (0.05% ethanol and 0.01% Silwet L-77). For the NPA experiment, the tissue was treated twice (at 0 and 7 h), as described previously (Nemhauser et al., 2000), with 100 μM NPA (in 0.1% dimethyl sulfoxide and 0.01% Silwet L-77) or a mock solution (0.1% dimethyl sulfoxide and 0.01% Silwet L-77) and collected 24 h after the initial treatment.

Plasmid Construction

For construction of the *ANT*:*GUS* plasmid, GUS and the 3′ nos terminator sequence were subcloned from pBI121 into pBluescript SK− using *Bam*HI and *Eco*RI and subsequently into pCGN1547 using *Bam*HI and *Hin*dIII. A 6.2-kb region of *ANT* sequence 5′ to the start codon was constructed in pBluescript SK− by first subcloning a 5-kb *ANT* genomic fragment followed by the addition of a 1.2-kb PCR product. The entire 6.2-kb *ANT* promoter sequence was subsequently subcloned upstream of GUS in pCGN1547 using *Kpn*I. *ANT*:*GUS*/pCGN1547 was transformed into *Agrobacterium tumefaciens* strain ASE by electroporation. Arabidopsis L*er* plants were transformed with this *Agrobacterium* strain by vacuum infiltration (Bechtold et al., 1993). Transformants were selected for kanamycin resistance.

The Arabidopsis Genome Initiative locus numbers for the genes analyzed in this article are as follows: *ANT*, At4g37750; *AIL6*, At5g10510; *AIL7*, At5g65510.

Supplemental Data

The following materials are available in the online version of this article.

Supplemental Figure S1. *ant ail6* flowers in mixed genetic backgrounds.

Supplemental Figure S2. *LFY* mRNA levels are not changed in *ant-4 ail6-2* inflorescences.

Supplemental Figure S3. *ant-4 ail6-2* leaves have altered leaf vein architecture.

Supplemental Figure S4. *ANT* expression is not altered after auxin treatment of inflorescences.

Supplemental Figure S5. *ANT*:*ANT* complements *ant-4*.

ACKNOWLEDGMENTS

I thank the Salk Institute Genomic Analysis Laboratory, the University of Wisconsin Arabidopsis knockout facility, and the GABI-Kat project for providing the Arabidopsis T-DNA insertion mutants used in this study. I thank the Arabidopsis Biological Resource Center for seeds of the T-DNA insertion alleles, Jennifer Fletcher for the *CLV3* and *WUS* plasmids used to generate in situ probes, Josefina Poupin for help with the *WUS* in situ hybridization experiments, Doris Wagner for the *LFY* plasmid used to generate an in situ probe and for *WUS*:*GUS* seeds, Gloria Muday and Gretchan Hagen for *AGH3-2*:*GUS* seeds, David Smyth for the pBW plasmid containing *ANT* genomic DNA, and Ben Scheres and Kalika Prasad for comments on the manuscript. I also acknowledge the University of South Carolina Electron Microscopy Center for instrument use and technical assistance.

Received May 8, 2009; accepted June 10, 2009; published June 19, 2009.

LITERATURE CITED

Aida M, Beis D, Heidstra R, Willemsen V, Blilou I, Galinha C, Nussaume L, Noh YS, Amasino R, Scheres B (2004) The *PLETHORA* genes mediate patterning of the Arabidopsis root stem cell niche. Cell **119:** 109–120

Alonso JM, Stepanova AN, Leisse TJ, Kim CJ, Chen H, Shinn P, Stevenson DK, Zimmerman J, Barajas P, Cheuk R, et al (2003) Genome-wide insertional mutagenesis of *Arabidopsis thaliana*. Science **301:** 653–657

Baker SC, Robinson-Beers K, Villanueva JM, Gaiser JC, Gasser CS (1997) Interactions among genes regulating ovule development in *Arabidopsis thaliana*. Genetics **145:** 1109–1124

Barbier de Reuille P, Bohn-Courseau I, Ljung K, Morin H, Carraro N, Godin C, Traas J (2006) Computer simulations reveal properties of the cell-cell signaling network at the shoot apex in Arabidopsis. Proc Natl Acad Sci USA **103:** 1627–1632

Bechtold N, Ellis J, Pelletier G (1993) In planta *Agrobacterium*-mediated gene transfer by infiltration of adult *Arabidopsis thaliana* plants. C R Acad Sci Ser III Sci Vie **316:** 1194–1199

Benjamins R, Scheres B (2008) Auxin: the looping star in plant development. Annu Rev Plant Biol **59:** 443–465

Benkova E, Michniewicz M, Sauer M, Teichmann T, Seifertova D, Jurgens G, Friml J (2003) Local, efflux-dependent auxin gradients as a common module for plant organ formation. Cell **115:** 591–602

Blazquez MA, Soowal LN, Lee I, Weigel D (1997) *LEAFY* expression and flower initiation in Arabidopsis. Development **124:** 3835–3844

Blilou I, Xu J, Wildwater M, Willemsen V, Paponov I, Friml J, Heidstra R, Aida M, Palme K, Scheres B (2005) The PIN auxin efflux facilitator network controls growth and patterning in Arabidopsis roots. Nature **433:** 39–44

Busch MA, Bomblies K, Weigel D (1999) Activation of a floral homeotic gene in *Arabidopsis*. Science **285:** 585–587

Das P, Ito T, Wellmer F, Vernoux T, Dedieu A, Traas J, Meyerowitz EM (2009) Floral stem cell termination involves the direct regulation of *AGAMOUS* by PERIANTHIA. Development **136:** 1605–1611

Deyholos MK, Sieburth LE (2000) Separable whorl-specific expression and negative regulation by enhancer elements within the *AGAMOUS* second intron. Plant Cell **12:** 1799–1810

Elliott RC, Betzner AS, Huttner E, Oakes MP, Tucker WQJ, Gerentes D, Perez P, Smyth DR (1996) *AINTEGUMENTA*, an *APETALA2*-like gene of *Arabidopsis* with pleiotropic roles in ovule development and floral organ growth. Plant Cell **8:** 155–168

Fleming AJ (2007) Plant signaling: the inexorable rise of auxin. Trends Cell Biol **16:** 397–402

Fletcher JC, Brand U, Running MP, Simon R, Meyerowitz EM (1999) Signaling of cell fate decisions by *CLAVATA3* in Arabidopsis shoot meristems. Science **283:** 1911–1914

Galinha C, Hofhuis H, Luijten M, Willemsen V, Blilou I, Heidstra R, Scheres B (2007) PLETHORA proteins as dose-dependent master regulators of Arabidopsis root development. Nature **449:** 1053–1057

Hames C, Ptchelkine D, Grimm C, Thevenon E, Moyroud E, Gerard F, Martiel JL, Benlloch R, Parcy F, Muller CW (2008) Structural basis for LEAFY floral switch function and similarity with helix-turn-helix proteins. EMBO J **27:** 2628–2637

Heisler MG, Ohno C, Das P, Sieber P, Reddy GV, Long JA, Meyerowitz EM (2005) Patterns of auxin transport and gene expression during primordium development revealed by live imaging of the *Arabidopsis* inflorescence meristem. Curr Biol **15:** 1899–1911

Hill TA, Day CD, Zondlo SC, Thackeray AG, Irish VF (1998) Discrete spatial and temporal cis-acting elements regulate transcription of the Arabidopsis floral homeotic gene *APETALA3*. Development **125:** 1711–1721

Hu Y, Xie A, Chua NH (2003) The *Arabidopsis* auxin-inducible gene *ARGOS* controls lateral organ size. Plant Cell **15:** 1951–1961

Jack T, Brockman LL, Meyerowitz EM (1992) The homeotic gene *APETALA3* of *Arabidopsis thaliana* encodes a MADS box and is expressed in petals and stamens. Cell **68:** 683–687

Kang J, Mizukami Y, Wang H, Fowke L, Dengler NG (2007) Modification of cell proliferation patterns alters leaf vein architecture in *Arabidopsis thaliana*. Planta **226:** 1207–1218

Klimyuk VI, Carroll BJ, Thomas CM, Jones JDG (1993) Alkali treatment for rapid preparation of plant material for reliable PCR analysis. Plant J **3:** 493–494

Klucher KM, Chow H, Reiser L, Fischer RL (1996) The *AINTEGUMENTA* gene of *Arabidopsis* required for ovule and female gametophyte development is related to the floral homeotic gene *APETALA2*. Plant Cell **8:** 137–153

Krizek BA (1999) Ectopic expression of *AINTEGUMENTA* in *Arabidopsis* plants results in increased growth of floral organs. Dev Genet **25:** 224–236

Krizek BA, Fletcher JC (2005) Molecular mechanisms of flower development: an armchair guide. Nat Rev Genet **6:** 688–698

Krizek BA, Meyerowitz EM (1996) The *Arabidopsis* genes *APETALA3* and *PISTILLATA* are sufficient to specify the B class organ identity function. Development **122:** 11–22

Krizek BA, Prost V, Macias A (2000) *AINTEGUMENTA* promotes petal identity and acts as a negative regulator of *AGAMOUS*. Plant Cell **12:** 1357–1366

Krysan PJ, Young JC, Sussman MR (1999) T-DNA as an insertional mutagen in *Arabidopsis*. Plant Cell **11:** 2283–2290

Lenhard M, Bohnert A, Jurgens G, Laux T (2001) Termination of stem cell maintenance in Arabidopsis floral meristems by interactions between *WUSCHEL* and *AGAMOUS*. Cell **105:** 805–814

Leyser O (2006) Dynamic integration of auxin transport and signalling. Curr Biol **16:** R424–R433

Liu Z, Franks RG, Klink VP (2000) Regulation of gynoecium marginal tissue formation by *LEUNIG* and *AINTEGUMENTA*. Plant Cell **12:** 1879–1891

Lohmann JU, Hong RL, Hobe M, Busch MA, Parcy F, Simon R, Weigel D (2001) A molecular link between stem cell regulation and floral patterning in Arabidopsis. Cell **105:** 793–803

Maier AT, Stehling-Sun S, Wollman H, Demar M, Hong RL, Haubeiss S, Weigel D, Lohmann JU (2009) Dual roles of the bZIP transcription factor PERIANTHIA in the control of floral architecture and homeotic gene expression. Development **136:** 1613–1620

Mayer KFX, Schoof H, Haecker A, Lenhard M, Jurgens G, Laux T (1998) Role of *WUSCHEL* in regulating stem cell fate in the Arabidopsis shoot meristem. Cell **95:** 805–815

Mizukami Y, Fischer RL (2000) Plant organ size control: *AINTEGUMENTA* regulates growth and cell numbers during organogenesis. Proc Natl Acad Sci USA **97:** 942–947

Nemhauser JL, Feldman LJ, Zambryski PC (2000) Auxin and *ETTIN* in *Arabidopsis* gynoecium morphogenesis. Development **127:** 3877–3888

Nole-Wilson S, Krizek BA (2000) DNA binding properties of the *Arabidopsis* floral development protein AINTEGUMENTA. Nucleic Acids Res **28:** 4076–4082

Nole-Wilson S, Krizek BA (2006) *AINTEGUMENTA* contributes to organ polarity and regulates growth of lateral organs in combination with *YABBY* genes. Plant Physiol **141:** 977–987

Nole-Wilson S, Tranby T, Krizek BA (2005) *AINTEGUMENTA*-like (*AIL*) genes are expressed in young tissues and may specify meristematic or division-competent states. Plant Mol Biol **57:** 613–628

Okada K, Ueda J, Komaki MK, Bell CJ, Shimura Y (1991) Requirement of the auxin polar transport system in early stages of *Arabidopsis* floral bud formation. Plant Cell **3:** 677–684

Parcy F, Nilsson O, Busch MA, Lee I, Weigel D (1998) A genetic framework for floral patterning. Nature **395:** 561–566

Prunet N, Morel P, Thierry A-M, Eshed Y, Bowman JL, Negrutiu I, Trehin C (2008) *REBELOTE, SQUINT,* and *ULTRAPETALA1* function redundantly in the temporal regulation of floral meristem termination in *Arabidopsis thaliana*. Plant Cell **20:** 901–919

Reinhardt D, Eva-Rachele P, Stieger P, Mandel T, Baltensperger K, Bennett M, Traas J, Friml J, Kuhlemeier C (2003) Regulation of phyllotaxis by polar auxin transport. Nature **426:** 255–260

Reinhardt D, Mandel T, Kuhlemeier C (2000) Auxin regulates the initiation and radial position of plant lateral organs. Plant Cell **12:** 507–518

Rosso MG, Li Y, Strizhov N, Reiss B, Dekker K, Weisshaar B (2003) An *Arabidopsis thaliana* T-DNA mutagenized population (GABI-Kat) for flanking sequence tag-based reverse genetics. Plant Mol Biol **53:** 247–259

Schruff MC, Spielman M, Tiwari S, Adams S, Fenby N, Scott RJ (2005) The *AUXIN RESPONSE FACTOR 2* gene of *Arabidopsis* links auxin signaling, cell division, and the size of seeds and other organs. Development **133:** 251–261

Sessions A, Burke E, Presting G, Aux G, McElver J, Patton D, Dietrich B, Ho P, Bacwaden J, Ko C, et al (2002) A high throughput Arabidopsis reverse genetics system. Plant Cell **14:** 2985–2994

Smith RS, Guyomarch S, Mandel T, Reinhardt D, Kuhlemeier C, Prusinkiewicz P (2006) A plausible model of phyllotaxis. Proc Natl Acad Sci USA **103:** 1301–1306

Tilly JJ, Allen DW, Jack T (1998) The CArG boxes in the promoter of the Arabidopsis floral organ identity gene *APETALA3* mediate diverse regulatory effects. Development **125:** 1647–1657

Vernoux T, Kronenberger J, Grandjean O, Laufs P, Traas J (2000) *PIN-FORMED 1* regulates cell fate at the periphery of the shoot apical meristem. Development **127:** 5157–5165

Verwoerd TC, Dekker BMM, Hoekema A (1989) A small scale procedure for the rapid isolation of plant RNAs. Nucleic Acids Res **17:** 2362

Weigel D, Alvarez J, Smyth DR, Yanofsky MF, Meyerowitz EM (1992) LEAFY controls floral meristem identity in Arabidopsis. Cell **69:** 843–859

Yanofsky MF, Ma H, Bowman JL, Drews GN, Feldman KA, Meyerowitz EM (1990) The protein encoded by the *Arabidopsis* homeotic gene *AGAMOUS* resembles transcription factors. Nature **346:** 35–39

Ye S, Dhillon S, Ke X, Collins AR, Day INM (2001) An efficient procedure for genotyping single nucleotide polymorphisms. Nucleic Acids Res **29:** e88